Activation of Conjunctiva-Associated Lymphoid Tissue in Patients With Infectious Keratitis Using In Vivo Confocal Microscopy

Yuting Liu,[1,2] Rui Zhu,[1,2] Xin Jin,[1,2] Yingbin Wang,[1,2] Yan Shi,[1,2] Nan Zhang,[1] Jingrao Wang,[1,2] Yueyan Dong,[1,2] and Hong Zhang[1,2]

[1]Eye Hospital, The First Affiliated Hospital of Harbin Medical University, Harbin City, Nangang District, Heilongjiang Province, Harbin, China
[2]Key Laboratory of Basic and Clinical Research of Heilongjiang Province, Heilongjiang Province, Harbin, China

PURPOSE. We aimed to evaluate activation of conjunctiva-associated lymphoid tissue (CALT) in patients with keratitis using in vivo confocal microscopy (IVCM) and conjunctival impression cytology (CIC).

METHODS. In addition to anterior segment photography and corneal fluorescein staining, IVCM revealed the palpebral conjunctiva in all subjects, and CIC and immunofluorescence staining were performed.

RESULTS. Diffuse lymphoid tissue cell density in the eyes of patients with keratitis was significantly greater compared with healthy volunteers ($P < 0.001$). Similar trends were found in perifollicular lymphocyte density ($P < 0.001$), follicular density ($P = 0.029$), follicular center reflection intensity ($P = 0.011$), and follicular area ($P < 0.001$). Immunofluorescence staining showed that the proportions of CD4$^+$ (61.7% ± 8.0% vs. 17.3% ± 10.2%, respectively, $P < 0.001$) and CD8$^+$ (46.9% ± 10.0% vs. 19.6% ± 11.5%, respectively, $P < 0.001$) cells in patients with keratitis was greater compared with healthy volunteers. Interestingly, we also observed changes in the contralateral eye in subjects with keratitis.

CONCLUSIONS. Our research suggests that CALT, as an ocular immune structure, is activated and plays an important role in the pathogenesis of keratitis. This has been overlooked previously. CALT is also active in the contralateral eye of subjects with keratitis.

Keywords: keratitis, conjunctiva-associated lymphoid tissue (CALT), in vivo confocal microscopy (IVCM)

Keratitis is one of the leading causes of blindness worldwide.[1] In addition to external stimulation by pathogens, immune responses, such as leukocyte infiltration, are an important factor causing corneal damage in patients with keratitis.[2,3] Leukocyte accumulation not only assists the body to eliminate harmful pathogens, but it also causes tissue damage. Leukocyte aggregation is facilitated by cytokines and chemokines, and T lymphocytes also play an important role in this process.[4] Researchers have found that in a model of *Pseudomonas aeruginosa* infection, infiltration of CD4$^+$ and CD8$^+$ T lymphocytes occurred in the cornea 3 and 5 days after infection, respectively.[5] After application of a CD4$^+$ T cell monoclonal antibody, the severity of keratitis decreased. In herpes stromal keratitis (HSK) infection, type 1 T helper (Th1) cell subtypes of CD4$^+$ T lymphocytes secreted cytokines, including interferon (IFN)-γ and interleukin (IL)-2, which led to an inflammatory response and angiogenesis, whereas CD8$^+$ T lymphocytes were related to formation of corneal scarring.[6]

Abundant evidence indicates that conjunctiva-associated lymphoid tissue (CALT) is an important functional unit for ocular immune protection.[7] CALT is composed of lymphoid follicles (afferent arm) and diffuse lymphoid tissue (efferent arm).[8] Diffuse lymphoid tissue distributes in the subepithelial lamina propria, which is mainly composed of lymphocytes and plasma cells.[9] Most of the lymphocytes are CD3$^+$ T cells; however, there is also a small proportion of CD20$^+$ B cells that secrete immunoglobulin (Ig)A.[9] Lymphoid follicles have typical structural features, including follicular-related epithelia and germinal centers. They are mainly composed of a large number of B cells in the center, which are surrounded by T cells.[9]

Knop et al. found that the most abundant area of CALT is the tarso-orbital area of the conjunctiva, rather than the bulbar conjunctiva or fornix conjunctiva in human autopsy specimens.[10] On the ocular surface in healthy humans, when the eyes are closed, the distribution of CALT in the upper tarsal conjunctiva corresponds to the position of the cornea.[11] Presence of a large number of plasma cells in CALT may be related to the protective effect of secretory IgA on the ocular surface, especially the cornea.[12] Through direct contact with the cornea, CALT may participate in corneal

immune protection against pathogens. However, this is yet to be confirmed.

Previous studies have suggested that ocular surface-related immune lesions are caused by immune cells derived from blood vessels and lymphatic vessels of the bulbar conjunctiva.[13] However, few studies have focused on CALT and corneal immunity. We speculate that CALT, as part of the lymph tissue covering the corneal surface, may play an important role in corneal immunity. We aimed to use in vivo confocal microscopy (IVCM) to determine whether CALT activation occurs during keratitis onset.

MATERIALS AND METHODS

We recruited 60 subjects diagnosed with infectious keratitis who were treated at the outpatient department of the First Affiliated Hospital of Harbin Medical University from October 2018 to July 2019, and 30 healthy volunteers without ocular disease. This study was approved by the Ethics Committee of the First Affiliated Hospital of Harbin Medical University (2020JS03) and adhered to the principles of the Helsinki Declaration.

Subjects

Subjects were included if they met one or more of the following inclusion criteria: (1) confocal microscopy or corneal scraping of the lesion area showed fungal hyphae or amoebic cysts; (2) positive results on bacterial culture; and (3) a diagnosis of infectious keratitis made by a corneal specialist according to medical history and symptoms, even if the above examinations revealed negative results.

The exclusion criteria included a history of ocular trauma; ocular surgery; autoimmune ocular diseases, such as graft-versus-host disease of the eye; and systemic diseases, such as diabetes mellitus. Patients who received systemic medications, such as glucocorticoids and immunosuppressive agents, at the time of examination were also excluded.

Subjects underwent a slit lamp examination, anterior segment photography, corneal fluorescein staining, IVCM, and conjunctiva impression cytology (CIC). In this study, both the infected eye and the contralateral eye of subjects with keratitis, as well as bilateral eyes of healthy volunteers, were examined. We performed the examination at the beginning of each patient's outpatient visit, and 51 patients were followed up 2 weeks after the initial visit during the course of treatment.

In Vivo Confocal Microscopy

The superior tarsal conjunctiva, which is the most widely distributed area of CALT, was examined using IVCM (Heidelberg Retinal Tomograph 3 with the Rostock Cornea Module; Heidelberg Engineering GmbH, Heidelberg, Germany), and IVCM images were collected for analysis. The examination was conducted as described previously. First, gel was added between the lens of the confocal microscope and the sterile cap (Tomo-Cap; Heidelberg Engineering GmbH) for coupling. IVCM provided images with fields of 400 × 400 μm. Oxybuprocaine hydrochloride eye drops (Benoxil 0.4%; Santen Pharmaceutical Co., Ltd., Japan) were administered once every 5 minutes 3 times for anesthesia. After patients received adequate anesthesia, corneal lesions and the superior tarsal conjunctiva were scanned layer by layer.

As described in previous literature, diffuse lymphocyte tissue is composed of diffusely distributed highly reflective cellular structures in the lamina propria, and lymphoid follicles are distributed beneath this diffuse lymphocyte layer. Lymphoid follicles are composed of oval structures with germinal centers, which are in turn surrounded by parafollicular lymphocytes. For each structure, three images from each eye with the best image quality were selected for analysis.

Image Analysis

Diffuse lymphocyte density, follicular density, and parafollicular lymphocyte density were manually measured using the Heidelberg cell counting software and IVCM. The image J software was used to calculate the area of lymphoid follicles and measure the gray value of follicular centers to determine reflection intensity.

CIC and Immunofluorescence Staining

After subjects received adequate topical anesthesia with oxybuprocaine hydrochloride eye drops, sterile membrane (0.45 μm; Millipore, Boston, MA, USA) was placed on the surface of the superior tarsal conjunctiva, gently pressed for 5 seconds, and then removed, and stored at −80°C.

Filter membranes were fixed with 4% paraformaldehyde for 1 hour. After washing with phosphate-buffered saline, filters were blocked with 0.1% Triton at room temperature for 20 minutes, and incubated with anti-CD4 antibody (A0362, 1:200; Abclonal, Wuhan, China) or anti-CD8 antibody (A11033, 1:200; Abclonal) at 4°C overnight, followed by incubation with Alexa Flour 488 anti-rabbit secondary antibody (A-11034, 1:1000; Invitrogen, Shanghai, China) for CD4 or Alexa Flour 594 anti-rabbit secondary antibody (A-11037, 1:1000; Invitrogen) for CD8 for 1 hour at room temperature. Stained samples were examined and photographed with a fluorescence microscope (LEICA DMi8; Leica Microsystems, Wetzlar, Germany) at 400 times magnification. Three fields of view for each sample were randomly chosen, and images were analyzed manually using Image J software to count DAPI$^+$ cells (blue, total cell number), CD4$^+$ cells (green), and CD8+ cells (red). Then, the percentage of CD4$^+$ DAPI$^+$ cells and CD8$^+$ DAPI$^+$ cells was calculated for subsequent statistical analysis.

Statistical Analysis

Data were analyzed using the SPSS software version 22.0 (SPSS Inc., IBM, Chicago, IL, USA). The Mann–Whitney U test was used to compare the ages of subjects with keratitis with healthy volunteers. The χ^2 test was used to analyze differences in sex between the two groups. The Mann–Whitney U test was used to compare diffuse lymphocyte density, follicular area, parafollicular lymphocyte density, reflection intensity of the follicular center, and follicular density. One-way analysis of variance was used to compare immunofluorescence staining results between the two groups. Wilcoxon's rank-sum test was used to analyze CALT-related parameters and the disease course. To identify differences in CALT parameters among different pathogen groups, the Kruskal–Wallis test was used. A P value of < 0.05 was considered statistically significant.

RESULTS

Demographics and Characteristics

A total of 60 subjects diagnosed with infectious keratitis, including bacterial keratitis ($n = 22$), fungal keratitis ($n = 16$), and HSK ($n = 22$), were enrolled in this study. Thirty healthy volunteers were also enrolled in the study. There was no statistically significant difference in age (45 years [Q25–Q75: 37–60 years] vs. 48 years [Q25–Q75: 41–57 years], $P = 0.593$) or sex (12 men, 18 women vs. 34 men, 26 women, $P = 0.136$) between the healthy group and the keratitis group. Representative examples of an anterior segment photograph and IVCM results are shown in Figure 1. Abundant neutrophil infiltration can be seen in the bacterial keratitis lesion, whereas there is a lack of typical pathogenic elements, such as fungal filaments (see Fig. 1D). In the affected area of eyes with fungal keratitis, a large number of highly reflective and linear fungal structures can be seen with irregular shapes and a large number of branches staggered in the cornea (see Fig. 1E). In HSK cornea, a large amount of dendritic cell infiltration in the basal epithelium and sub-epithelial nerve plexus can be seen (see Fig. 1F).

Changes in CALT-Related Parameters in the Eyes of Subjects With Keratitis

The distribution depth of diffuse lymphoid tissue ranged from 10 to 30 μm. Diffuse lymphoid tissue consisted of a layered structure composed of intraepithelial lymphocytes in the conjunctival epithelium and lymphocytes in the lamina propria. Confocal microscopy images showed irregularly shaped highly reflective cells. In the eyes of subjects with keratitis, the diffuse lymphocyte density increased significantly compared with healthy volunteers (1426 cells/mm^2 [Q25–Q75: 860–2272 cells/mm^2] vs. 192 cells/mm^2 [Q25–Q75: 140–254 cells/mm^2], respectively, $P < 0.001$; Figs. 2, 3).

Lymphoid follicles were located underneath the epithelial layer (20–80 μm) and were composed of germinal centers and parafollicular lymphocytes. In the eyes of subjects with keratitis, follicular area was significantly greater compared with healthy volunteers (36,284 mm^2 [Q25–Q75: 27,204–44,080 mm^2] vs. 21,947 mm^2 [Q25–Q75: 17,493–25,451 mm^2], respectively, $P < 0.001$), the reflection intensity of the lymphoid follicular center was higher (119 [Q25–Q75: 104–138] vs. 107 [Q25–Q75: 96–118], respectively, $P = 0.011$), and the follicular densities (28 follicles/mm^2 [Q25–Q75: 24–35 follicles/mm^2] vs. 26 follicles/mm^2 [Q25–Q75: 24–30 follicles/mm^2], respectively, $P = 0.029$) and the density of parafollicular lymphocytes (406 cells/mm^2 [Q25–Q75: 345–608 cells/mm^2] vs. 131 cells/mm^2 [Q25–Q75: 102–151 cells/mm^2], respectively, $P < 0.001$) increased (Figs. 2, 4). In addition, we analyzed CALT-related parameters among patients with bacterial, fungal, and viral keratitis. We found no significant difference among the three groups (Table 1).

Changes in CD4$^+$ and CD8$^+$ Cells in the Eyes of Subjects With Keratitis

After performing CIC on the superior tarsal conjunctiva in subjects with keratitis and healthy volunteers, we performed CD4$^+$ and CD8$^+$ immunofluorescence staining with filters. The results show that the percentage of CD4$^+$ (61.7% ± 8.0% vs. 17.3% ± 10.2%, respectively, $P < 0.001$) and CD8$^+$ (46.9% ± 10.0% vs. 19.6% ± 11.5%, respectively, $P < 0.001$) cells increased significantly in the eyes of subjects with keratitis compared with healthy volunteers (Figs. 5, 6).

Changes in CALT-Related Parameters in the Contralateral Eye of Subjects With Keratitis

The diffuse lymphocyte density in the contralateral eye of subjects with infectious keratitis was significantly greater
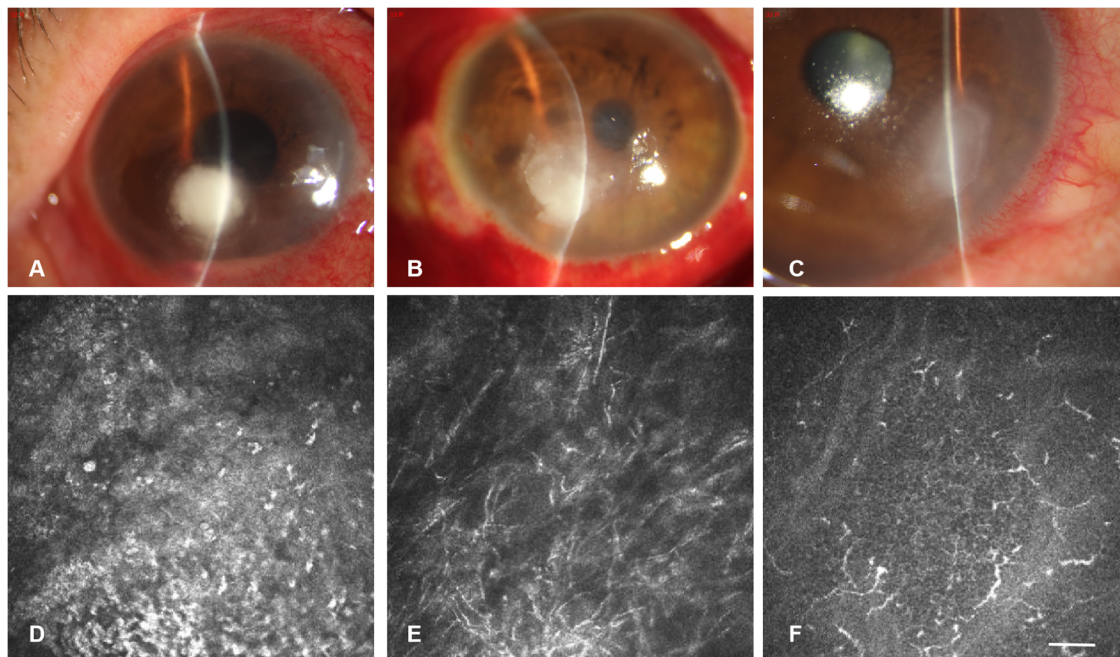

FIGURE 1. Representative anterior segment photographs of the cornea in a subject with infectious keratitis. (**A, D**) Anterior segment photographs and in vivo confocal microscopy (IVCM) images of bacterial keratitis. (**B, E**) Anterior segment photographs and IVCM images of fungal keratitis. (**C, F**) Anterior segment photograph and IVCM images of viral keratitis. Scale bar: 50 μm.
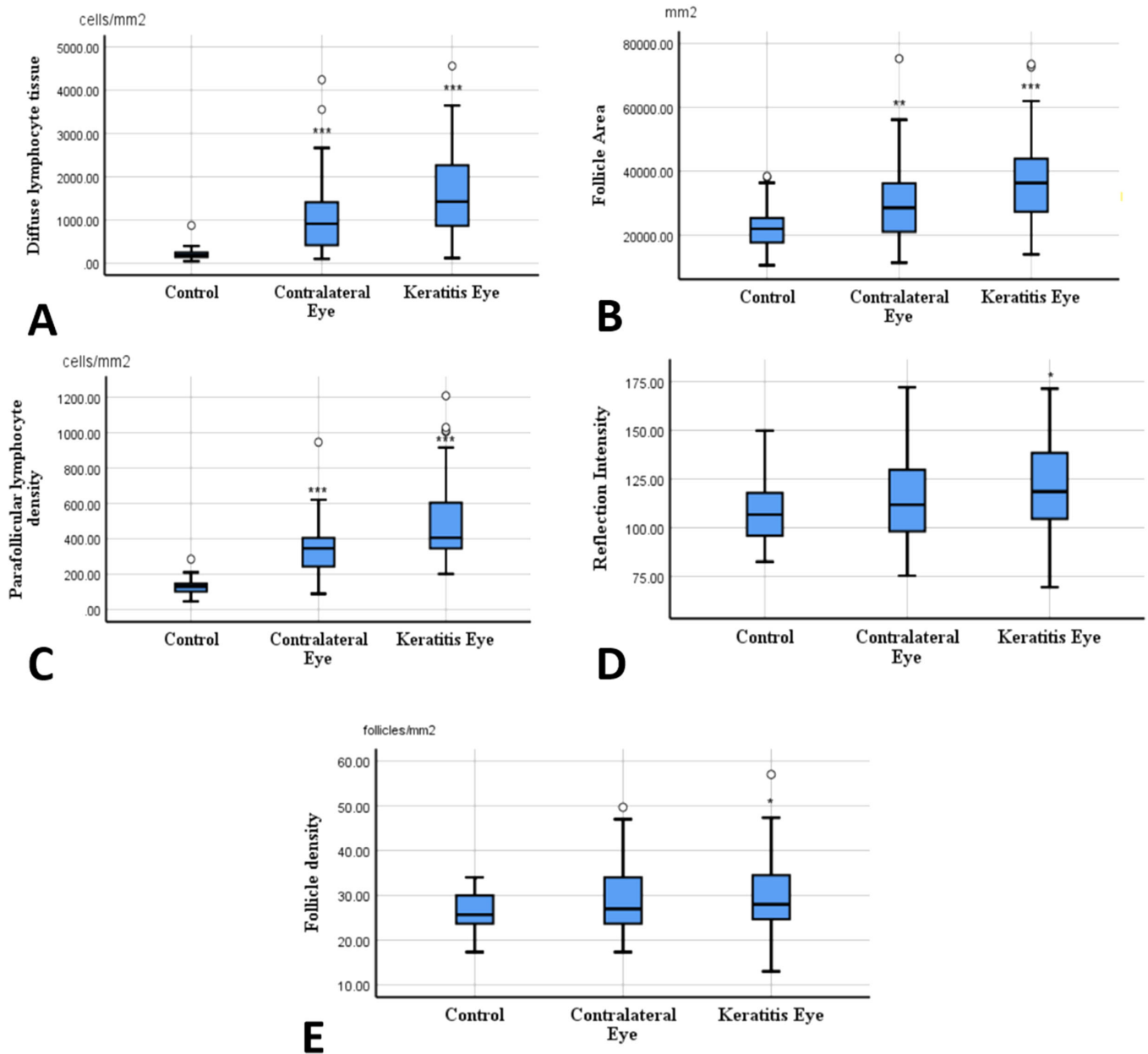
FIGURE 2. Diffuse lymphocyte density, parafollicular lymphocyte density, and follicular area of eyes with keratitis and contralateral eyes are significantly greater compared with eyes from healthy volunteers. Follicular density and reflection intensity in eyes affected by keratitis are higher compared with eyes from healthy volunteers, whereas related parameters in the contralateral eye are not significantly different between groups (***$P < 0.001$ compared with healthy volunteers; **$P < 0.01$ compared with healthy volunteers; *$P < 0.05$ compared with healthy volunteers).

compared with healthy volunteers (910 cells/mm² [Q25–Q75: 413–1430 cells/mm²] vs. 192 cells/mm² [Q25–Q75: 140–254 cells/mm²], respectively, $P < 0.001$). Follicle-related parameters, including parafollicular lymphocyte density (346 cells/mm² [Q25–Q75: 243–407 cells/mm²] vs. 131 cells/mm² [Q25–Q75: 102–151 cells/mm²], respectively, $P < 0.001$) and follicular area (28,531 mm² [Q25–Q75: 20,966–36,317 mm²] vs. 21,947 mm² [Q25–Q75: 17,493–25,451 mm²], respectively, $P = 0.003$), also increased significantly. However, there was no significant difference in follicular density (27 follicles/mm² [Q25–Q75: 24–34 follicles/mm²] vs. 26 follicles/mm² [Q25–Q75: 24–30 follicles/mm²], respectively, $P = 0.069$; Figs. 2, 7) or follic-

ular center reflection intensity (112 [Q25–Q75: 98–130] vs. 107 [Q25–Q75: 96–118], respectively, $P = 0.349$) between the contralateral eyes of subjects with keratitis and those of healthy volunteers.

Changes in CD4⁺ and CD8⁺ Cells in the Contralateral Eyes of Subjects With Keratitis

We analyzed CD4⁺ and CD8⁺ data from CIC samples of the contralateral eye of subjects with keratitis. CD4⁺ (57.5% ± 8.0% vs. 17.3% ± 10.2%, respectively, $P < 0.001$) and CD8⁺ (45.2% ± 15.1% vs. 19.6% ± 11.5%, respectively,
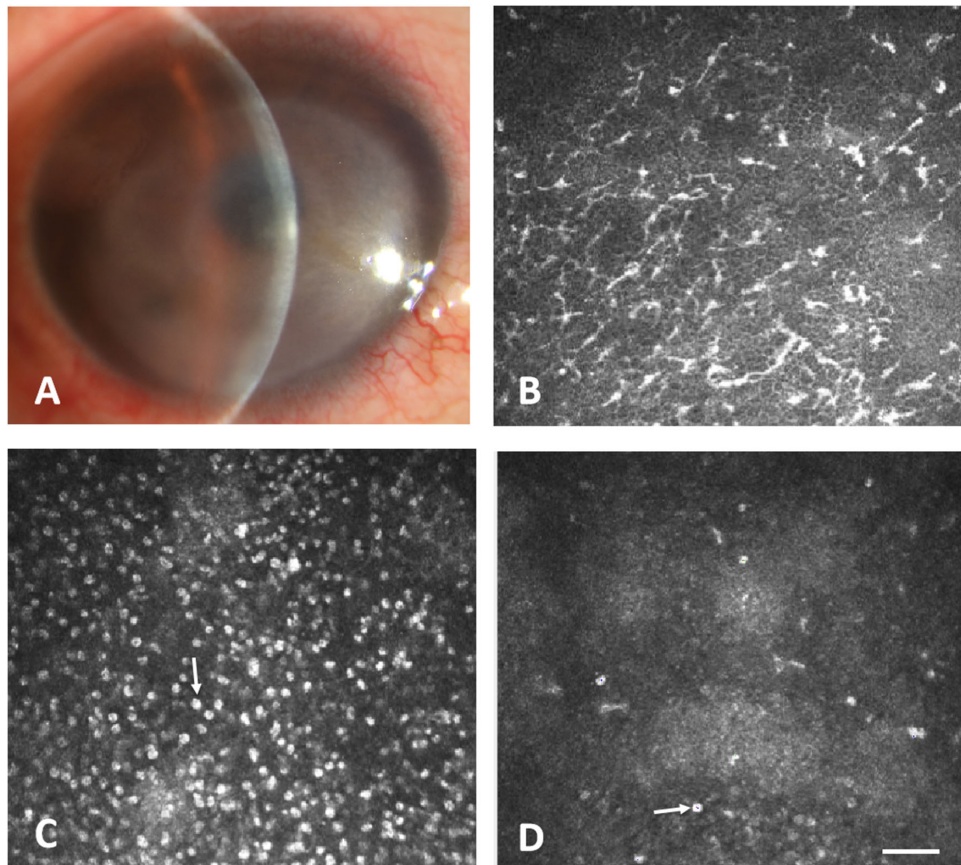
FIGURE 3. (**A, B**) Anterior segment photograph and in-vivo confocal microscopy (IVCM) images of a subject with infectious keratitis. (**C**) IVCM image of diffuse lymphoid tissue in a subject with diffuse keratitis, showing a large number of irregularly shaped and highly reflective cells, which were regarded as lymphocytes. (**D**) IVCM image of diffuse lymphoid tissue from a healthy volunteer. The density of highly reflective cells is significantly lower compared with the subject with keratitis. Scale bar: 50 µm.

$P < 0.001$) cells in CIC samples from contralateral eyes were significantly more abundant in subjects with keratitis compared with healthy volunteers. There was no significant difference in $CD4^+$ ($P = 0.969$) or $CD8^+$ ($P = 0.782$) cells in contralateral eyes compared with affected eyes (see Fig. 6).

Activation of CALT Changes With Disease Course

Of the 60 subjects with keratitis, 51 were followed up at 2 weeks. Among them, 35 subjects showed an improvement, whereas 16 subjects showed deterioration. During follow-up observation of subjects with keratitis, some CALT parameters changed as the disease progressed or improved. When treatment improved the condition, after 2 weeks, certain parameters, including diffuse lymphocyte density (1696 cells/mm² [Q25–Q75: 1166–2572 cells/mm²] vs. 782 cells/mm² [Q25–Q75: 351–1316 cells/mm²], respectively, $P < 0.001$), parafollicular lymphocyte density (439 cells/mm² [Q25–Q75: 345–683 cells/mm²] vs. 295 cells/mm² [Q25–Q75: 238–452 cells/mm²], respectively, $P = 0.001$), and follicular area (39,263 mm² [Q25–Q75: 28,743–44,940 mm²] vs. 22,983 mm² [Q25–Q75: 18,578–32,003 mm²], respectively, $P < 0.001$) in CALT decreased compared with 2 weeks prior (Fig. 8, Table 2). When the condition deteriorated, diffuse lymphocyte density (932 cells/mm² [Q25–Q75: 453–1733 cells/mm²] vs. 1338 cells/mm² [Q25–Q75: 954–1810 cells/mm²], respec-

tively, $P = 0.023$) and parafollicular lymphocyte density (390 cells/mm² [Q25–Q75: 317–503 cells/mm²] vs. 597 cells/mm² [Q25–Q75: 417–855 cells/mm²], respectively, $P = 0.004$) increased significantly (Fig. 9, Table 3).

DISCUSSION

Infectious keratitis is a leading cause of blindness worldwide.[1] To our knowledge, this is the first study to assess changes in CALT in subjects with infectious keratitis using IVCM. When compared with healthy volunteers, the diffuse lymphocyte density in the infected and contralateral eyes of subjects with infectious keratitis was significantly increased, follicular area was significantly reduced, the reflection intensity of the follicular center was significantly enhanced, and parafollicular lymphocyte density was significantly increased. Immunofluorescence staining of CIC samples of the palpebral conjunctiva showed that the proportion of $CD4^+$ and $CD8^+$ cells was significantly greater in subjects with keratitis compared with healthy volunteers. The above results indicate that CALT plays an important role in the pathogenesis of keratitis.

cIn recent years, our understanding of CALT has gradually improved. After performing a large number of autopsies, Knop et al. confirmed that CALT has similar structural features to other mucosa-associated lymphoid tissues,
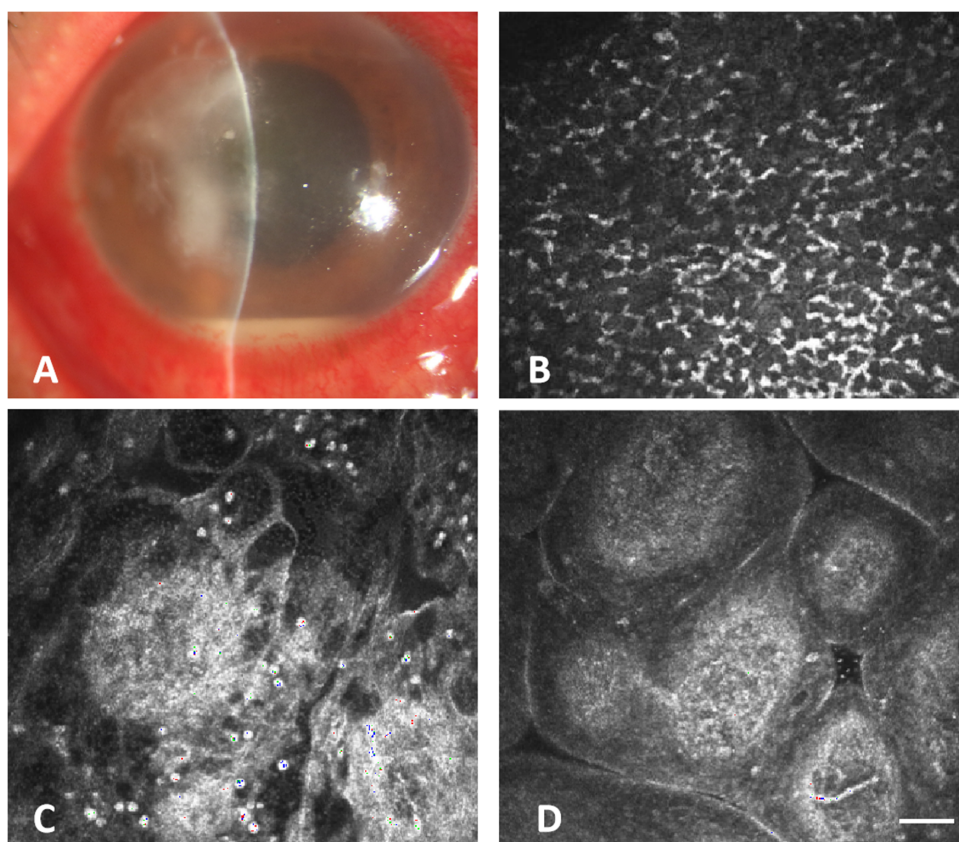
FIGURE 4. (**A, B**) Anterior segment photograph and in-vivo confocal microscopy (IVCM) images of a patient with infectious keratitis. (**C**) IVCM image of a lymphoid follicle in a subject with infectious keratitis. (**D**) Lymphoid follicles from a healthy volunteer. Lymphoid follicles affected by infectious keratitis show a greater number of parafollicular lymphocytes, a larger follicular area, and a brighter follicular center compared with unaffected follicles. Scale bar: 50 µm.

TABLE 1. Analysis of CALT-Related Parameters Among Subjects With Keratitis Caused by Different Pathogens

	Bacterial Keratitis ($n = 22$) Median (Q25–Q75)	HSK ($n = 22$) Median (Q25–Q75)	Fungal Keratitis ($n = 16$) Median (Q25–Q75)	Z	P Value
Diffuse lymphocyte density (cells/mm^2)	1541 (501, 2351)	1041 (768, 2052)	1923 (1209, 2320)	2.330	0.312
Follicular area (mm^2)	33491 (25,258, 42,326)	39,727 (30,677, 47,989)	32,469 (26,143, 43,130)	3.475	0.176
Parafollicular lymphocyte density (cells/mm^2)	388 (313, 615)	456 (361, 703)	393 (349, 579)	1.266	0.531
Follicular center reflection intensity	122 (108, 139)	110 (101, 146)	113 (102, 138)	0.589	0.745
Follicular density (follicles/mm^2)	26 (26, 34)	29 (24, 36)	30 (24, 34)	0.051	0.975

CALT, conjunctiva-associated lymphoid tissue; HSK, herpes stromal keratitis.

consisting of diffuse lymphoid tissue, lymphoid follicles, and high endothelial venules.[9] Diffuse lymphoid tissue is located in the lamina propria of tarsal and orbital conjunctiva, and is mainly composed of T lymphocytes, IgA, and plasma cells.[9] Diffuse lymphoid tissue forms the efferent arm of the ocular surface's immune protection. Lymphoid follicles have an oval shape with a germinal center composed of CD20$^+$ B lymphocytes in the center, with T lymphocytes distributed around this germinal center.[9] Lymphoid follicles form the afferent arm of CALT. CALT is mainly located at the tarsal and orbital conjunctiva, and its distribution covers the corneal surface when the eyelid is closed.[11] Therefore, it can be speculated that the afferent arm of CALT detects corneal antigens and mediates the corresponding immune response, whereas the efferent arm secretes IgA and cytokines to protect the cornea.

The role of CALT in the pathogenesis of corneal disease remains unknown. After applying lipopolysaccharide to rabbit eyes, Liang et al. observed that inflammatory cell infiltration in CALT tissues increased significantly, as did the number of CD45$^+$ lymphocytes.[14] Agnifili performed IVCM on 108 healthy volunteers and found that CALT is a normal structure in healthy humans, whereas the related parameters change with age.[15] In our study, a significant increase in diffuse lymphocyte density and changes in follicular parameters in subjects with keratitis indicated that CALT is activated during keratitis onset, which is consistent with the changing trend of CALT in previous studies. As keratitis improved, ocular surface inflammation gradually reduced, and diffuse lymphoid tissue and follicle-related changes also settled.

In HSK, CD4$^+$ T lymphocytes mediate a series of inflammatory reactions.[16] CD4$^+$ T lymphocyte infiltration occurs in
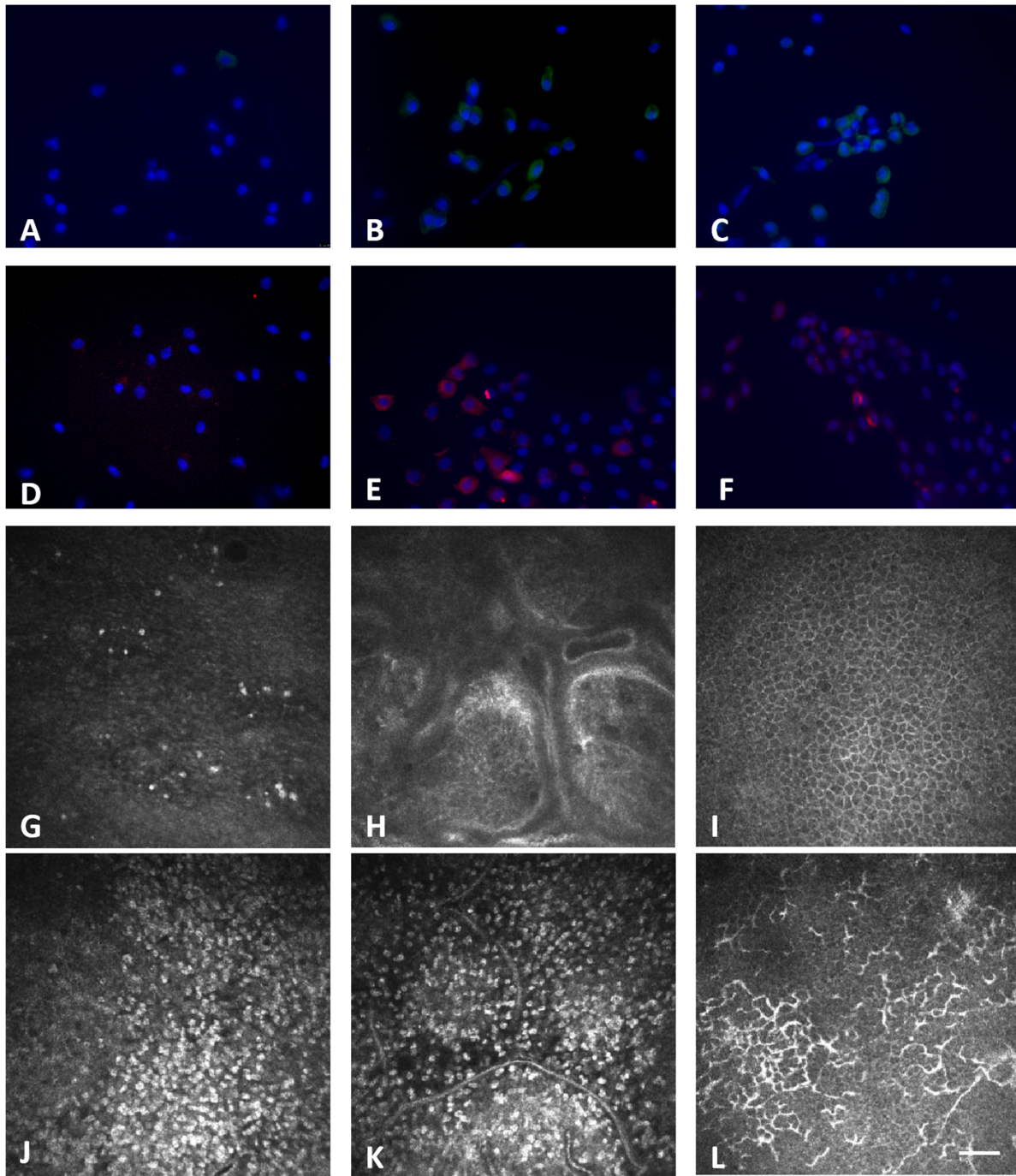
FIGURE 5. Immunofluorescence staining of conjunctival impression cytology (CIC) samples and corresponding in vivo confocal microscopy (IVCM) images of the same subjects. (**A**) CD4$^+$ immunofluorescence staining (*green*) using CIC samples from a healthy volunteer. (**B**) CD4$^+$ immunofluorescence staining using CIC samples from a subject with keratitis. (**C**) CD8$^+$ immunofluorescence staining (*red*) using CIC samples from a healthy volunteer. (**D**) CD8$^+$ immunofluorescence staining using CIC samples from a subject with keratitis. (**G, H, I**) IVCM images of diffuse lymphoid tissue, lymphoid follicles, and the cornea in a healthy volunteer. (**J, K, L**) IVCM images of diffuse lymphoid tissue, lymphoid follicles, and the cornea in a subject with keratitis. Magnification: × 400. Scale bar: 50 µm.

the cornea approximately 6 days after animals are infected with herpes simplex virus.[17] Infiltrated CD4$^+$ T lymphocytes mainly differentiate into Th1 and Th17 cell subtypes.[18] The Th1 subtype of cells release pro-inflammatory cytokines, such as IL-2 and IFN-γ, and this process aids viral elimination.[18] In addition, a large number of Th17 cells also infiltrate the cornea of HSK animal models, which is

accompanied by increased IL-17 levels.[19] Systemic application of anti-IL-17 antibodies significantly reduces the degree of keratitis and CD4$^+$ T lymphocyte infiltration.[19] Moreover, CD8$^+$ T lymphocytes play a protective role in the inflammatory process in response to HSK infection.[20] Stuart et al. found that in HSK animal models lacking CD8$^+$ T lymphocytes, keratitis was more severe.[21]
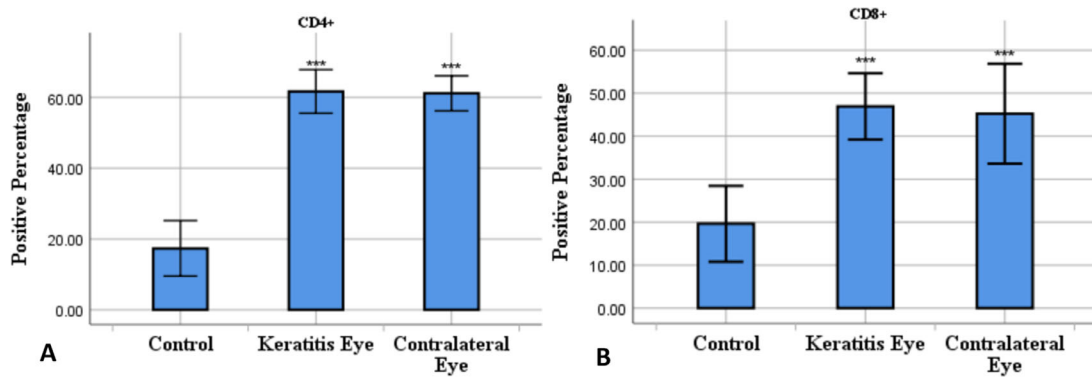
FIGURE 6. The percentage of cells positive for CD4$^+$ or CD8$^+$ is higher in keratitis eyes and contralateral eyes from subjects with keratitis compared with healthy volunteers ($^{***}P < 0.001$).
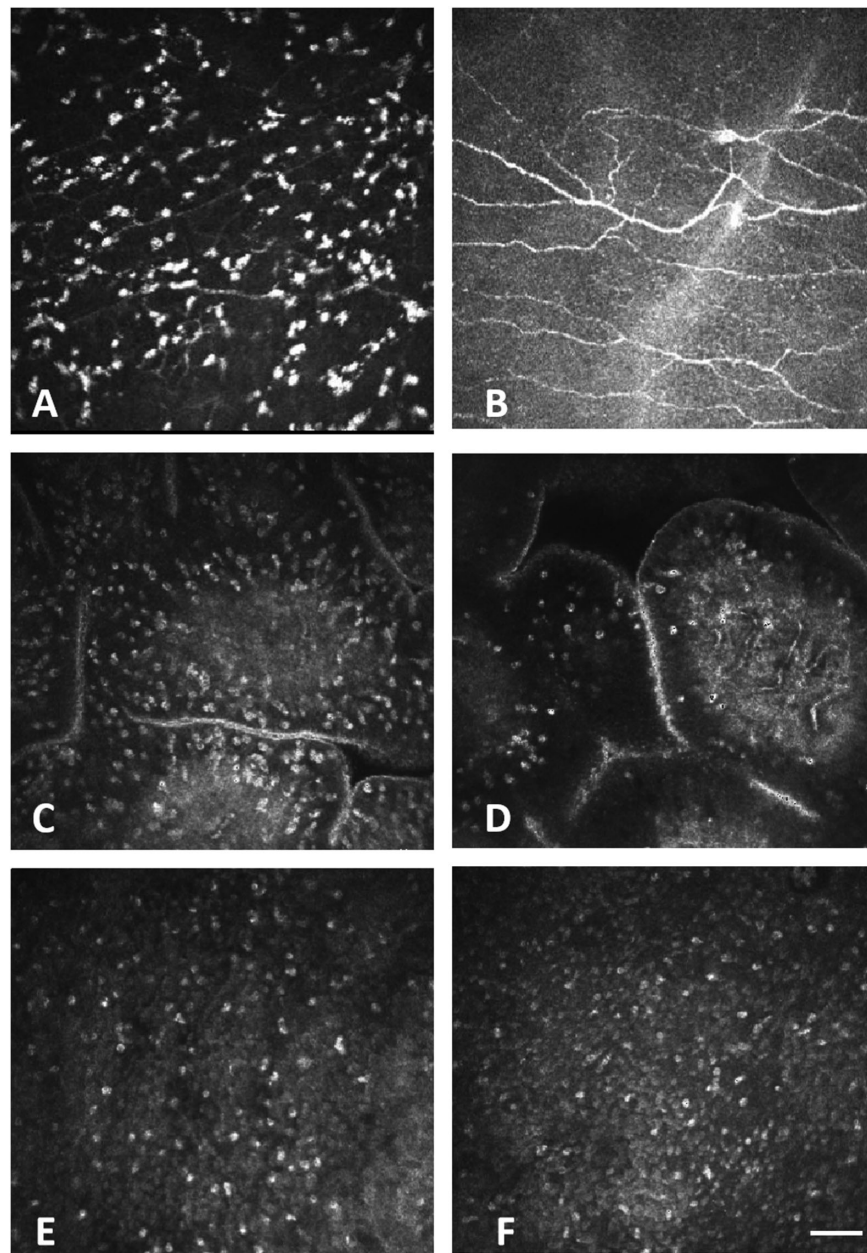

FIGURE 7. (**A, B**) Invivo confocal microscopy (IVCM) photograph of a subject with monocular infectious keratitis in the affected eye **A** and contralateral eye **B**. (**C, D**) IVCM photograph of lymphoid follicles in the affected eye **C** and the contralateral eye **D**. (**E, F**) IVCM photograph of diffuse lymphoid tissue in the affected eye (**E**) and the contralateral eye (**F**). Scale bar: 50 μm.
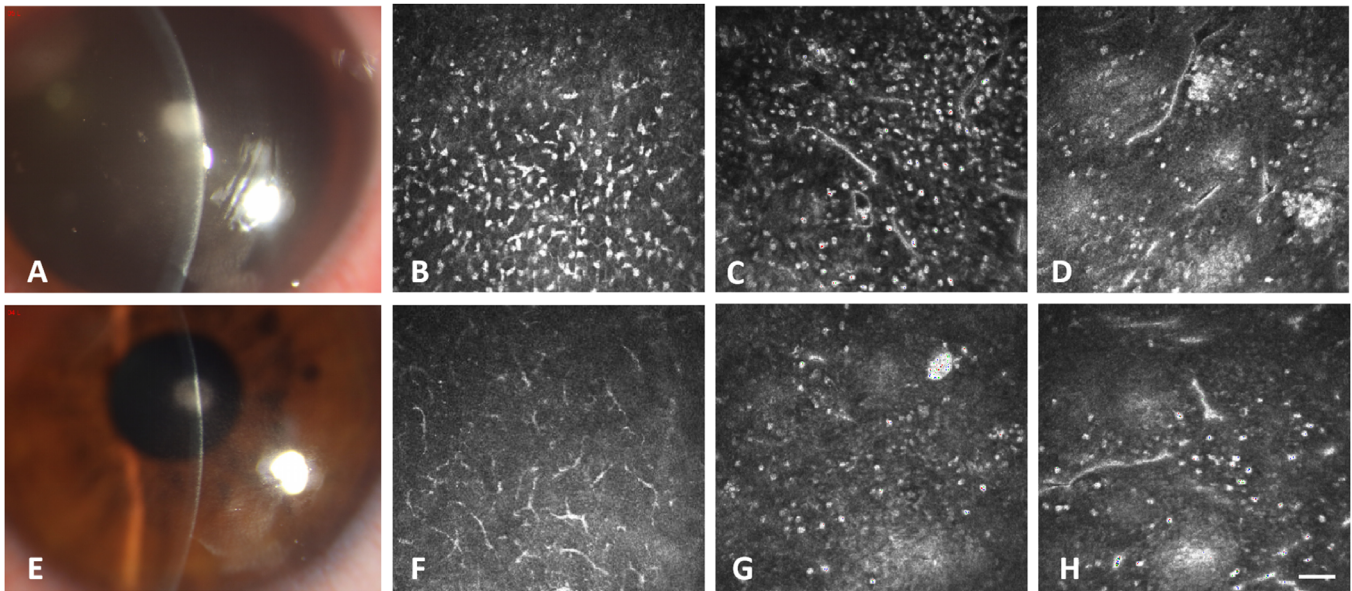
FIGURE 8. (**A, E**) Anterior segment photographs of a patient with keratitis before and after treatment. (**B, F**) In-vivo confocal microscopy (IVCM) photographs of an eye with keratitis before and after treatment. (**C**) IVCM results of diffuse lymphocytes before treatment. (**D**) IVCM results of lymphoid follicles before treatment. (**G**) IVCM results of diffuse lymphocytes after treatment. (**H**) IVCM results of lymphoid follicles after treatment. Compared with before treatment **A**, keratitis improved, the lesion was localized, corneal edema was reduced **E**, and diffuse lymphocyte **C, G** and parafollicular lymphocyte **D, H** density were reduced. Scale bar: 50 µm.

TABLE 2. Analysis of CALT-Related Parameters in Subjects With an Improvement in Keratitis

	Initial Visit Median (Q25–Q75)	Two-Week Follow-up Median (Q25–Q75)	Z	P Value
Diffuse lymphocyte density (cells/mm^2)	1696 (1166, 2572)	782 (351, 1316)	−5.143	**<0.001**
Follicular area (mm^2)	39,263 (28,743, 44,940)	22,983 (18,578, 32,003)	−3.653	**<0.001**
Parafollicular lymphocyte density (cells/mm^2)	439 (345, 683)	295 (238, 452)	−3.431	**0.001**
Follicular center reflection intensity	114 (103, 138)	116 (102, 123)	−0.753	0.451
Follicular density (follicles/mm^2)	26 (21, 32)	25 (19, 30)	−1.574	0.116

CALT, conjunctiva-associated lymphoid tissue.

Similarly, CD4$^+$ and CD8$^+$ T lymphocytes infiltrated the cornea on the third and fifth days after *P. aeruginosa* keratitis infection, respectively.[22] After CD4$^+$ T lymphocytes were cleared from the cornea of rats, the severity of corneal lesions was significantly reduced, and the occurrence of corneal perforation was also reduced after application of a neutralizing antibody against the Th1 cytokine, IFN-γ.[5]

In animal models of *Fusarium solani* infection, Hu et al. found that the levels of CD4$^+$ and CD8$^+$ T lymphocytes in corneal and draining lymph nodes were significantly increased.[23] In keratitis caused by *Candida albicans*, researchers found that the level of IL-17 in the cornea was significantly increased, and a large amount of IL-17 was secreted by CD4$^+$ T cells, but the cornea of BALB/c mice with depleted CD4$^+$ T cells did not manifest typical candidal keratitis lesions. This result indicates that CD4$^+$ T lymphocytes play an essential role in the pathogenesis of fungal keratitis.[24]

The results of the abovementioned studies indicate that CD4$^+$ and CD8$^+$ T lymphocytes are widely involved in the pathogenesis of infectious keratitis caused by different pathogens, including bacteria, fungi, and viruses.[21,24,25]

However, ophthalmologists and scientists mostly focus on the involvement of CD4$^+$ and CD8$^+$ T lymphocytes in keratitis disease only in the cornea; no attention has been paid to the changes in immune cells in the tarsal conjunctiva. As a mucosal lymphoid tissue covering the corneal surface, whether CALT participates in the pathogenesis of keratitis has not previously been investigated. At present, our article is the only study to examine this.

We also analyzed the CALT-related parameters of keratitis caused by different pathogens. However, we did not identify any differences in CALT-related parameters among subjects with keratitis caused by different pathogens. In the future, specific changes in CALT in subjects with keratitis caused by different pathogens need to be further explored in clinical experiments and animal models.

In our study, we found that CALT was in an activated state in both eyes in subjects with keratitis, which is consistent with the results of previous studies on the immune status of both eyes during keratitis onset. Multiple diseases and operations involving only one eye often lead to a series of changes in the contralateral eye. After unilateral cataract surgery, an inflammatory response, including elevated monocyte chemoattractant protein-1 and transform-
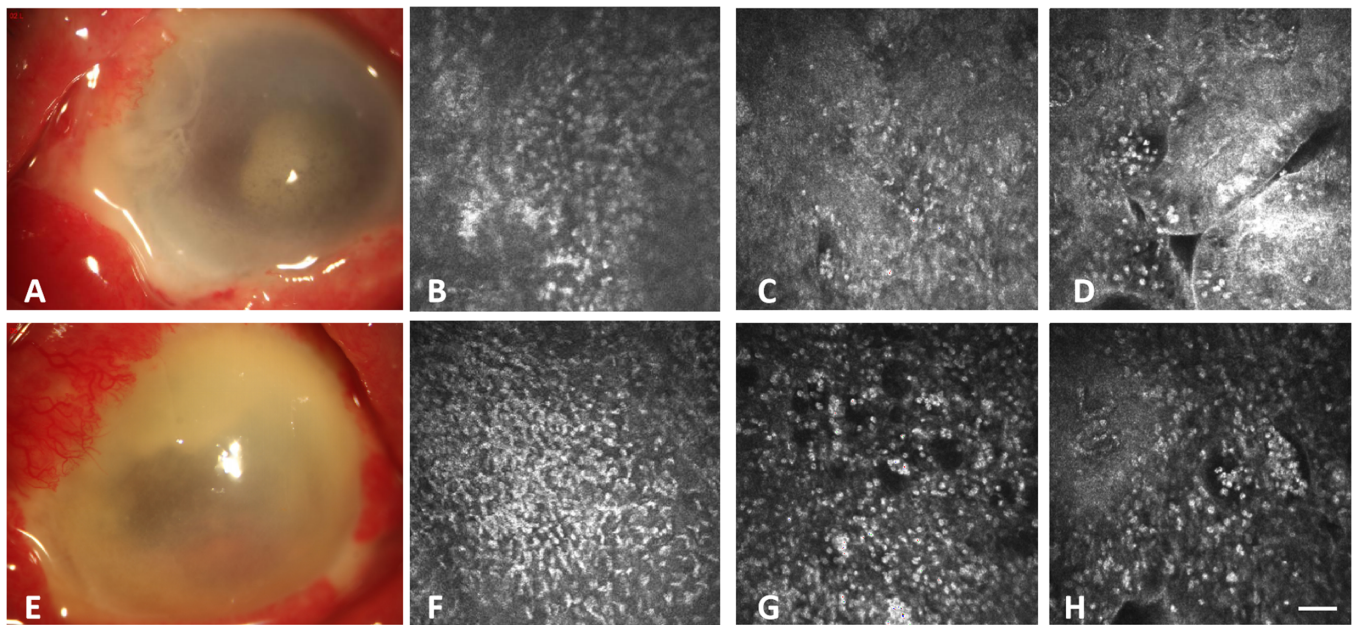
FIGURE 9. (**A, E**) Anterior segment photographs from the same patient with uncontrolled keratitis before and after 2 weeks of treatment. (**B, F**) In vivo confocal microscopy (IVCM) photographs of the uncontrolled eye before and after treatment. Compared with the IVCM image of diffuse lymphocytes (**C**) and parafollicular lymphocytes (**D**) 2 weeks before treatment, diffuse lymphocyte (**G**) and parafollicular lymphocyte (**H**) density increased as keratitis deteriorated. Scale bar: 50 µm.

TABLE 3. Analysis of CALT-Related Parameters in Subjects With a Deterioration in Keratitis

	Initial Visit Median (Q25–Q75)	Two-Week Follow-up Median (Q25–Q75)	Z	P Value
Diffuse lymphocyte density (cells/mm^2)	932 (453, 1733)	1338 (954, 1810)	−2.275	**0.023**
Follicular area (mm^2)	33,799 (24,463, 42,652)	33,796 (22,796, 44,624)	−0.155	0.877
Parafollicular lymphocyte density (cells/mm^2)	390 (317, 503)	597 (417, 855)	−2.844	**0.004**
Follicular center reflection intensity	124 (106, 138)	125 (98, 137)	−0.931	0.352
Follicular density (follicles/mm^2)	30 (26, 36)	32 (26, 40)	−0.979	0.328

CALT, conjunctiva-associated lymphoid tissue.

ing growth factor β2, occurs in the aqueous humor of the contralateral eye.[26,27] In infectious keratitis and neurotrophic keratitis, the contralateral eye shows a decrease in nerve density in the sub-basal nerve plexus[28,29]; however, the specific mechanism of these changes is still unclear. We speculate that immune and neurological factors participate jointly in CALT activation in the contralateral eye of subjects with keratitis. On the one hand, the body's mucosal immune system is interconnected. Bienenstock found that mesenteric lymph node-derived IgA and B cells specifically migrate to all mucosa-associated lymphoid tissues, including bronchus-associated lymphoid tissue, gut-associated lymphoid tissue, and urogenital-associated lymphoid tissue.[30] Therefore, it can be speculated that the mucosal immune system is inter-related. However, neurological factors also play an important role in this process. Cruzat et al. performed IVCM on the contralateral eye of subjects with infectious keratitis and found that the number of dendritic cells in the cornea of the contralateral eye increased significantly compared with the control group.[31] This process was accompanied by a decrease in the density of subepithelial nerve fibers in the contralateral cornea.[32] In addition, cytokine levels, such as IL-2, IL-10, and IL-17 levels, increased in tears from contralateral

eyes of subjects with infectious keratitis.[33] It can be speculated that pathogenic infection causes nerve fibers under the corneal epithelium to release sensory neuropeptides, which act on immune cell. This in turn leads to immune cell infiltration and activation, including dendritic cell infiltration and activation, in the cornea. T lymphocyte differentiation and function can also be influenced by cytokine secretion.[34,35]

The above results show that the body's mucosal immune system is interconnected. When one mucosa-associated lymphoid tissue (MALT) site is stimulated by a pathogen, other MALT sites may be subsequently activated.[36] Therefore, when one side of the cornea is infected by pathogens and CALT is activated, CALT in the contralateral eye may be activated immediately through an interconnection between mucosal immune systems.

Our study has some limitations that should be noted. First, the follow-up period was short. In future studies, we will further extend the follow-up period to make more detailed observations of long-term changes in CALT. In addition, whether activation of CALT with different lesions is related to the clinical score of keratitis remains to be investigated. These shortcomings should be clarified in future research.

CONCLUSIONS

In conclusion, our study confirmed activation of CALT in both eyes of subjects with keratitis by examination of the palpebral conjunctiva using IVCM. The degree of CALT activation gradually decreased as the ocular condition improved. Immunofluorescence staining of CIC samples showed that CD4$^+$ and CD8$^+$ T lymphocytes are activated during this process. Therefore, CALT plays an extremely important role in the pathogenesis of infectious diseases of the ocular surface, especially infectious keratitis.

Disclosure: **Y. Liu**, None; **R. Zhu**, None; **X. Jin**, None; **Y. Wang**, None; **Y. Shi**, None; **N. Zhang**, None; **J. Wang**, None; **Y. Dong**, None; **H. Zhang**, None

References

1. Whitcher JP, Srinivasan M, Upadhyay MP. Corneal blindness: a global perspective. *Bull World Health Organ*. 2001;79:214–221.
2. Rajasagi NK, Rouse BT. The Role of T Cells in Herpes Stromal Keratitis. *Front Immunol*. 2019;10:512.
3. Strieter RM, Standiford TJ, Huffnagle GB, Colletti LM, Lukacs NW, Kunkel SL. "The good, the bad, and the ugly." The role of chemokines in models of human disease. *J Immunol*. 1996;156:3583–3586.
4. Hazlett LD. Corneal response to Pseudomonas aeruginosa infection. *Prog Retin Eye Res*. 2004;23:1–30.
5. Kwon B, Hazlett LD. Association of CD4$^+$ T cell-dependent keratitis with genetic susceptibility to Pseudomonas aeruginosa ocular infection. *J Immunol*. 1997;159:6283–6290.
6. Niemiałtowski MG, Rouse BT. Predominance of Th1 cells in ocular tissues during herpetic stromal keratitis. *J Immunol*. 1992;149:3035–3039.
7. Franklin RM, Remus LE. Conjunctival-associated lymphoid tissue: evidence for a role in the secretory immune system. *Invest Ophthalmol Vis Sci*. 1984;25:181–187.
8. Steven P, Gebert A. Conjunctiva-associated lymphoid tissue - current knowledge, animal models and experimental prospects. *Ophthalmic Res*. 2009;42:2–8.
9. Knop N, Knop E. Conjunctiva-associated lymphoid tissue in the human eye. *Invest Ophthalmol Vis Sci*. 2000;41:1270–1279.
10. Knop N, Knop E. The crypt system of the human conjunctiva. *Adv Exp Med Biol*. 2002;506:867–872.
11. Knop E, Knop N. The role of eye-associated lymphoid tissue in corneal immune protection. *J Anat*. 2005;206:271–285.
12. Knop E, Knop N, Claus P. Local production of secretory IgA in the eye-associated lymphoid tissue (EALT) of the normal human ocular surface. *Invest Ophthalmol Vis Sci*. 2008;49:2322–2329.
13. Niederkorn JY. High-risk corneal allografts and why they lose their immune privilege. *Curr Opin Allergy Clin Immunol*. 2010;10:493–497.
14. Liang H, Baudouin C, Dupas B, Brignole-Baudouin F. Live conjunctiva-associated lymphoid tissue analysis in rabbit under inflammatory stimuli using in vivo confocal microscopy. *Invest Ophthalmol Vis Sci*. 2010;51:1008–1015.
15. Agnifili L, Mastropasqua R, Fasanella V, et al. In vivo confocal microscopy of conjunctiva-associated lymphoid tissue in healthy humans. *Invest Ophthalmol Vis Sci*. 2014;55:5254–5262.
16. Newell CK, Martin S, Sendele D, Mercadal CM, Rouse BT. Herpes simplex virus-induced stromal keratitis: role of T-lymphocyte subsets in immunopathology. *J Virol*. 1989;63:769–775.
17. Biswas PS, Rouse BT. Early events in HSV keratitis–setting the stage for a blinding disease. *Microbes Infect*. 2005;7:799–810.
18. Xu M, Lepisto AJ, Hendricks RL. CD154 signaling regulates the Th1 response to herpes simplex virus-1 and inflammation in infected corneas. *J Immunol*. 2004;173:1232–1239.
19. Xia L, Zhang S, Cao Z, Hu Y, Yang H, Wang D. Interleukin-17 enhanced immunoinflammatory lesions in a mouse model of recurrent herpetic keratitis. *Microbes Infect*. 2013;15:126–139.
20. Doymaz MZ, Rouse BT. Herpetic stromal keratitis: an immunopathologic disease mediated by CD4$^+$ T lymphocytes. *Invest Ophthalmol Vis Sci*. 1992;33:2165–2173.
21. Stuart PM, Summers B, Morris JE, Morrison LA, Leib DA. CD8(+) T cells control corneal disease following ocular infection with herpes simplex virus type 1. *J Gen Virol*. 2004;85:2055–2063.
22. Hazlett LD, McClellan S, Kwon B, Barrett R. Increased severity of Pseudomonas aeruginosa corneal infection in strains of mice designated as Th1 versus Th2 responsive. *Invest Ophthalmol Vis Sci*. 2000;41:805–810.
23. Hu J, Hu Y, Chen S, et al. Role of activated macrophages in experimental Fusarium solani keratitis. *Exp Eye Res*. 2014;129:57–65.
24. Zhang H, Li H, Li Y, et al. IL-17 plays a central role in initiating experimental Candida albicans infection in mouse corneas. *Eur J Immunol*. 2013;43:2671–2682.
25. Buela K-AG, Hendricks RL. Cornea-infiltrating and lymph node dendritic cells contribute to CD4+ T cell expansion after herpes simplex virus-1 ocular infection. *J Immunol*. 2015;194:379–387.
26. Zhu X-J, Wolff D, Zhang K-K, et al. Molecular inflammation in the contralateral eye after cataract surgery in the first eye. *Invest Ophthalmol Vis Sci*. 2015;56:5566–5573.
27. Gong X, Ren Y, Fang X, Cai J, Song E. Substance P induces sympathetic immune response in the contralateral eye after the first eye cataract surgery in type 2 diabetic patients. *BMC Ophthalmology*. 2020;20:339.
28. Giannaccare G, Pellegrini M, Taroni L, et al. Longitudinal morphometric analysis of sub-basal nerve plexus in contralateral eyes of patients with unilateral neurotrophic keratitis. *Current Eye Research*. 2019;44:1047–1053.
29. Hamrah P, Cruzat A, Dastjerdi MH, et al. Unilateral herpes zoster ophthalmicus results in bilateral corneal nerve alteration: an in vivo confocal microscopy study. *Ophthalmology*. 2013;120:40–47.
30. McDermott MR, Bienenstock J. Evidence for a common mucosal immunologic system. I. Migration of B immunoblasts into intestinal, respiratory, and genital tissues. *J Immunol*. 1979;122:1892–1898.
31. Cruzat A, Schrems WA, Schrems-Hoesl LM, et al. Contralateral clinically unaffected eyes of patients with unilateral infectious keratitis demonstrate a sympathetic immune response. *Invest Ophthalmol Vis Sci*. 2015;56:6612–6620.
32. Yamaguchi T, Calvacanti BM, Cruzat A, et al. Correlation between human tear cytokine levels and cellular corneal changes in patients with bacterial keratitis by in vivo

confocal microscopy. *Invest Ophthalmol Vis Sci*. 2014; 55:7457–7466.

33. Agro A, Stanisz AM. Neuroimmunomodulation: classical and non-classical cellular activation. *Adv Neuroimmunol*. 1995;5:311–319.

34. Holzer P. Local effector functions of capsaicin-sensitive sensory nerve endings: involvement of tachykinins, calcitonin gene-related peptide and other neuropeptides. *Neuroscience*. 1988;24:739–768.

35. Hosoi J, Murphy GF, Egan CL, et al. Regulation of Langerhans cell function by nerves containing calcitonin gene-related peptide. *Nature*. 1993;363:159–163.

36. Imaoka K, Miller CJ, Kubota M, et al. Nasal immunization of nonhuman primates with simian immunodeficiency virus p55gag and cholera toxin adjuvant induces Th1/Th2 help for virus-specific immune responses in reproductive tissues. *J Immunol*. 1998;161:5952–5958.